

Parametric decomposition of optic flow by humans

José F. Barraza^{a,*}, Norberto M. Grzywacz^b

^a *Departamento de Luminotecnia, Luz y Visión, Universidad Nacional de Tucumán, and Consejo Nacional de Investigaciones Científicas y Técnicas, Av. Independencia 1800, 4000 San Miguel de Tucumán, Tucumán, Argentina*

^b *Department of Biomedical Engineering, Neuroscience Graduate Program, and Center for Vision Science and Technology, University of Southern California, University Park DRB 140, Los Angeles, CA 90089-1111, USA*

Received 30 April 2004; received in revised form 3 January 2005

Abstract

Ego motion and natural motions in the world generate complex optic flows in the retina. These optic flows, if produced by rigid surface patches, can be decomposed into four components, including rotation and expansion. We showed previously that humans can precisely estimate parameters of these components, such as the angular velocity of a rotational motion and the rate of expansion of a radial motion. However, natural optic flows mostly display motions containing a combination of more than one of these components. Here, we report that when a pure motion (e.g., rotation) is combined with its orthogonal component (e.g., expansion), no bias is found in the estimate of the component parameters. This suggests that the visual system can decompose complex motions. However, this decomposition is such that the presence of the orthogonal component increases the discrimination threshold for the original component. We propose a model for how the brain decomposes the optic flow into its elementary components. The model accounts for how errors in the estimate of local-velocity vectors affect the decomposition, producing the increase of discrimination thresholds.

© 2005 Published by Elsevier Ltd.

Keywords: Motion; Optic flow; Parametric decomposition; Internal noise; Discrimination

1. Introduction

When objects move or one moves through the environment, an *optic flow* is generated on our retinas. This flow contains valuable information about our position and movement in the world, and about its three-dimensional structure (Gibson, 1950; Koenderink & van Doorn, 1976). Koenderink and van Doorn showed that small planar patches of surfaces generate optic flows that one can decompose in terms of a few elementary motions, including translation, expansion, and rotation. The brain may take advantage of such theoretical decomposition by incorporating these elementary components as models for the analysis of motions in natural

scenes (Yuille & Grzywacz, 1998). Experimental justification for this hypothesis comes from psychophysical experiments showing the existence of looming and rotation detectors (Freeman & Harris, 1992; Morrone, Burr, & Vaina, 1995; Regan & Beberley, 1978, 1985; Snowden & Milne, 1995) working independently (Kappers, van Doorn, & Koenderink, 1994; Te Pas, Kappers, & Koenderink, 1996), and from physiological studies showing that there are cortical neurons sensitive to translation, rotation, expansion, and spiral motion (Duffy & Wurtz, 1991a, 1991b; Graziano, Andersen, & Snowden, 1994; Lagae, Maes, Raiguel, Xiao, & Orban, 1994; Maunsell & Van Essen, 1983; Tanaka, Fukuda, & Saito, 1989; Tanaka & Saito, 1989). However, the use of internal models for the analysis of visual motion requires that these specialized neural mechanisms work parametrically. For example, a parametric model for

* Corresponding author. Tel./fax: +54 381 4361936.
E-mail address: jbarraza@herrera.unt.edu.ar (J.F. Barraza).

rotation would have a center of rotation and an angular velocity as parameters to be determined. Previous experiments showed that humans can precisely estimate parameters of translational motions such as direction (De Bruyn & Orban, 1988) and speed (Johnston, Benton, & Morgan, 1999; McKee, 1981). More recently, we extended these findings to other elementary components of the optic flow, such as rotation and radial motion. We found that humans can estimate the angular velocity of rotation (Barraza & Grzywacz, 2002, 2004) and the rate of expansion of radial motion (Wurfel, Barraza, & Grzywacz, 2003). However, these experiments used pure rotations and expansions. And natural optic flows rarely contain such pure basic motion components in isolation from each other.

Can the brain estimate the parameters of the models from optic flows containing a combination of more than one of these components? This might be possible if it could decompose the motion into the elementary components. Such a decomposition is an issue of particular theoretical relevance, as raised by Yuille and Grzywacz (1998). A decomposition like this would only make sense if the mechanisms measuring the different motion components were sufficiently independent. Previous investigations have shown that mechanisms detecting radial and rotational motions are independent from each other (Freeman & Harris, 1992; Meese & Harris, 2001; Te Pas et al., 1996) and independent from that detecting translational motion (Kappers et al., 1994; Regan & Beberley, 1978, 1985; Te Pas et al., 1996). In this article, we show that this independence in the motion-detection mechanisms extends to the suprathreshold estimate of the motion-component parameters. These findings on optic-flow decomposition into independent components appeared in abstract form elsewhere (Barraza & Grzywacz, 2003a, 2003b).

2. Methods

2.1. Stimulus

Stimuli consisted of random-dot patterns undergoing either spiral motion or pure rotation, displayed in a circular patch whose diameter was 20° . Fig. 1 shows an example of a stimulus undergoing spiral motion; line segments indicate the flow of the pattern, with their lengths being proportional to the speeds of the dots. The dot density (191 dot deg^{-2}) was homogeneous across the field. The size of the dots was $11'$ and they were displayed with a luminance of 19.5 cdm^{-2} on a background whose luminance was 39 cdm^{-2} . They each had a finite lifetime of three frames. To avoid coherent flicker, only a third of the dots died between two frames. Random-dot patterns were displayed on a high-resolution CRT monitor at a frame rate of 75 Hz.

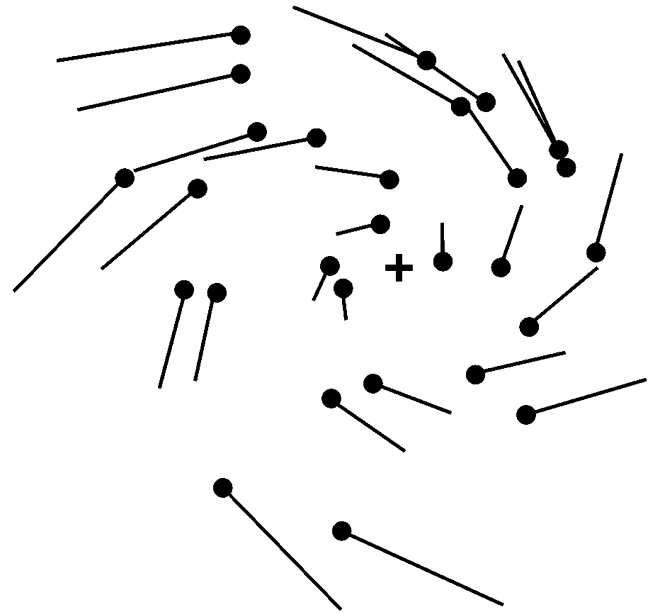


Fig. 1. Schematic of a random-dot pattern undergoing spiral motion. Line segments indicate the flow of the pattern, with their lengths being proportional to the speed of the dots.

2.2. Procedure

We performed three different kinds of motion-discrimination experiments. In the first experiment, we measured how subjects estimate either angular velocity or rate of expansion, and measured thresholds for motion-rate discrimination from spiral motions. One of the components of these motions (rotation or expansion) was the component of interest, whereas the orthogonal stimuli component acted as a mask. We presented to the subjects two motion stimuli (reference and test) into two temporally separated intervals. In each trial, each of the two stimuli was assigned its own random value of the mask, which was applied to the whole display.

Consequently, the mask caused all dots in a stimulus to move consistently with the same spiral. With this mask randomization, we prevented subjects from performing the matching task by using local speeds. The distribution of the mask values across trials was homogeneous and thus, we chose to indicate in our plots the range of values that the mask could reach in each trial. They were defined in terms of local speeds. A value m meant that for each position in the display, the speed of the orthogonal component of the motion was m times the speed of the component of interest.

In each trial of this first experiment, subjects had to indicate by pressing a button of the mouse which stimulus, reference or test, was moving faster. The order of presentation of the reference and test stimuli was random. We required subjects to ignore the mask component of the stimulus motion and make the comparison based on the component of interest. For instant, when

the component of interest was rotation, subjects had to ignore the radial motion to perform the task. We used a two-alternative forced-choice paradigm with the

method of constant stimuli to obtain the subjects' psychometric functions. Rates of motion in the constant stimuli were defined in terms of proportions of that

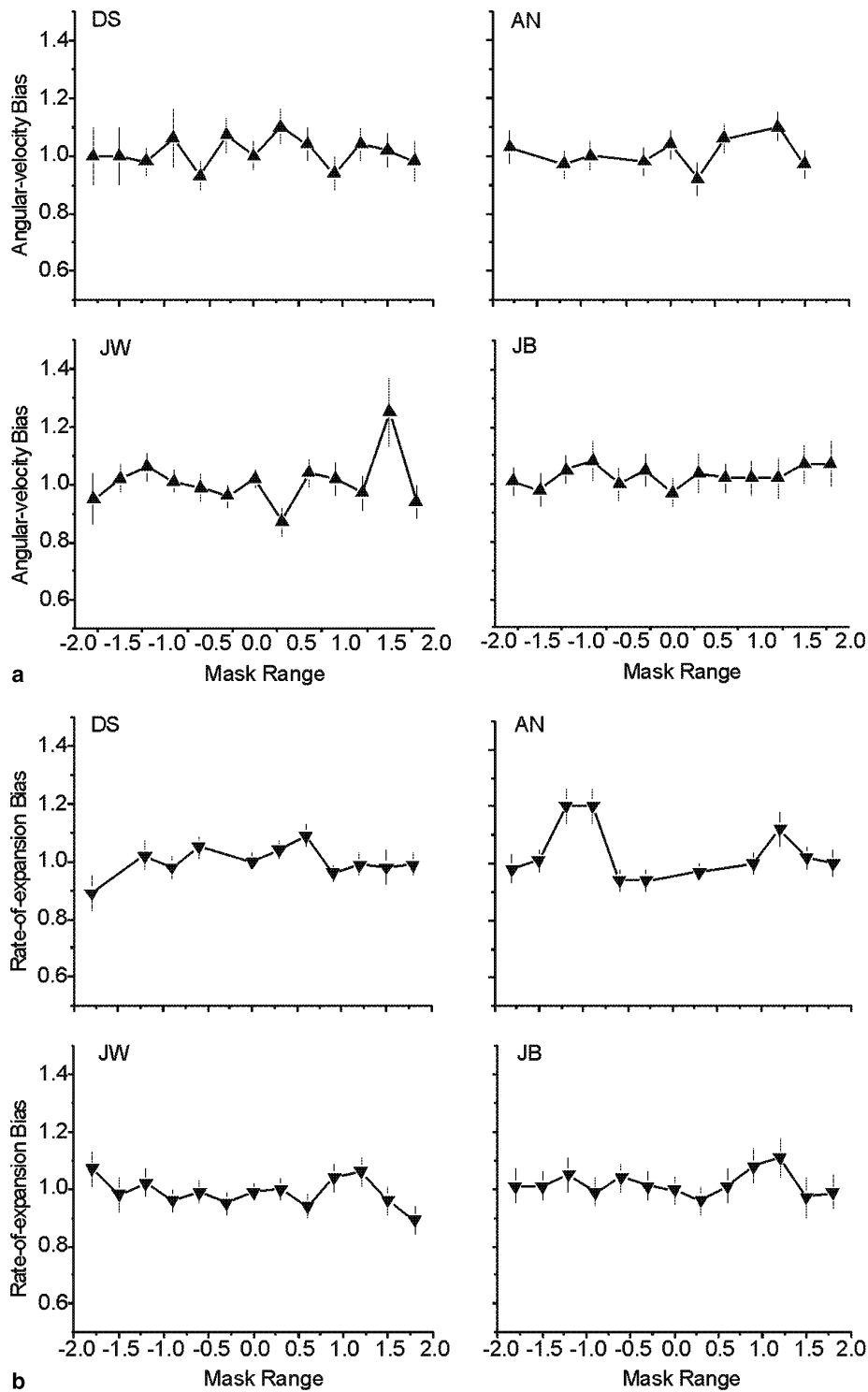


Fig. 2. Motion-rate bias as a function of the mask range for four subjects. In (a, b), rotation and radial motion are the motion components of interest, respectively. The results show that the combination of a basic motion component with its orthogonal component does not induce any bias in the perception of their motion-rate. Hence the visual system appears to use sufficiently independent mechanisms to decompose the optic flow into basic components, which include rotation and radial motion.

of the reference. The matching motion rate and the discrimination threshold were calculated by fitting cumulative Gaussian curves to these functions. The matching motion rate corresponded to their 50% point, while discrimination thresholds were calculated from the difference between the motion rate at 75% performance and the matching motion rate. To obtain the psychometric functions, a set of six stimuli was used in each block of trials. Each stimulus appeared a total of twenty times per block.

In the second experiment, the mask was applied only to the test stimulus and had a fixed value. Again, we measured the bias in the estimation of angular velocity and rate of expansion with orthogonal components.

In the third experiment, we investigated the effect of adding noise to the directions of local motions on the estimate of angular velocity. To do this, we rotated the velocity vector of each dot in a pure rotation by a random angle. The distribution of angles was Gaussian, with its standard deviation being the independent variable of the experiment. Angles in the test stimuli were computed frame by frame (which means that dots changed their direction every frame), whereas the reference stimulus was noise-free. Subjects had to compare the angular velocity of a noisy test against a non-noisy reference, with a procedure identical to that used in the first experiment.

Both experiments were carried out using a reference motion rate of 1 s^{-1} .

2.3. Subjects

Six subjects participated in these experiments, one of the authors and five others naïve as to the purpose of the study. Subjects viewed the display binocularly, with natural pupils.

3. Results

We measured the bias in the estimate of either angular velocity or rate of expansion, when combining rotations and radial motions with each other to produce spiral motions. In addition to the bias, we measured the discrimination threshold for both angular velocity and rate of expansion. The bias is defined as the ratio between perceived and actual (reference) motion rates of the component of interest. Because the perceived motion rate is defined in terms of a proportion of that of the reference, the bias is measured directly from the matching motion rate. This rate is the inverse of the bias.

Fig. 2 shows the bias as a function of the mask range (Section 2), when the motion of interest is rotation (a) or radial motion (b). The results indicate that the presence of the orthogonal component of motion does not produce any bias in the estimate of angular velocity or of rate of expansion. This suggests that the visual system can decompose the spiral motion, and estimate the parameters of rotation and radial motion independently.

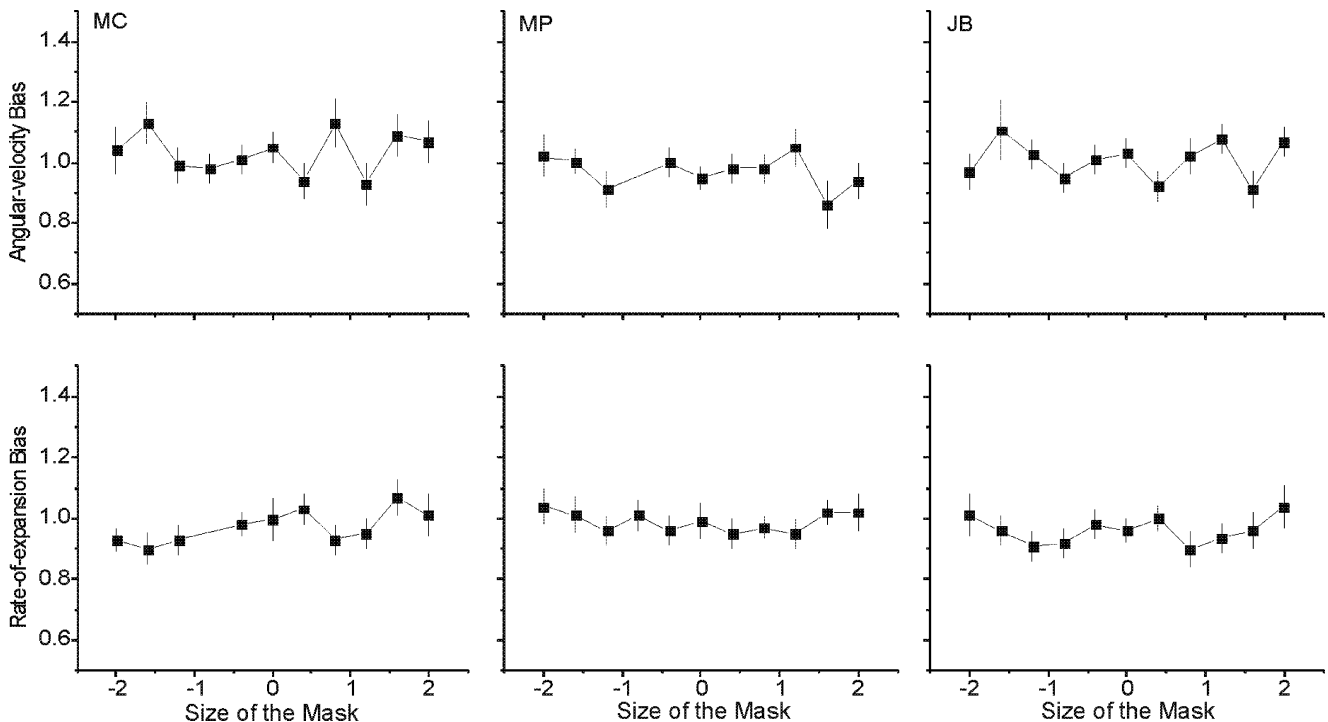


Fig. 3. Motion-rate bias as a function of the fixed size of the mask relative to the component of interest for three subjects. Conventions in this figure are similar to Fig. 2, except that here, the mask has fixed size and is only for the test stimulus. Fig. 3 confirms the results of the first experiment.

A possible complication with the conclusion that the visual system decomposes rotation and radial motion is that a mask with higher velocities is added sometimes to the reference and sometimes to the test. This addition is random and occurs with equal probability. Hence, a possible mask bias may cancel out along trials, not appearing in the results. Another problem could arise,

because in each block of trials, the size of the mask is chosen from a range between zero and a maximum. Results could thus be averaging together data for large-mask and small-mask differences with data for small mask differences.

We performed a control experiment to test whether the randomization of the mask caused a problem. This

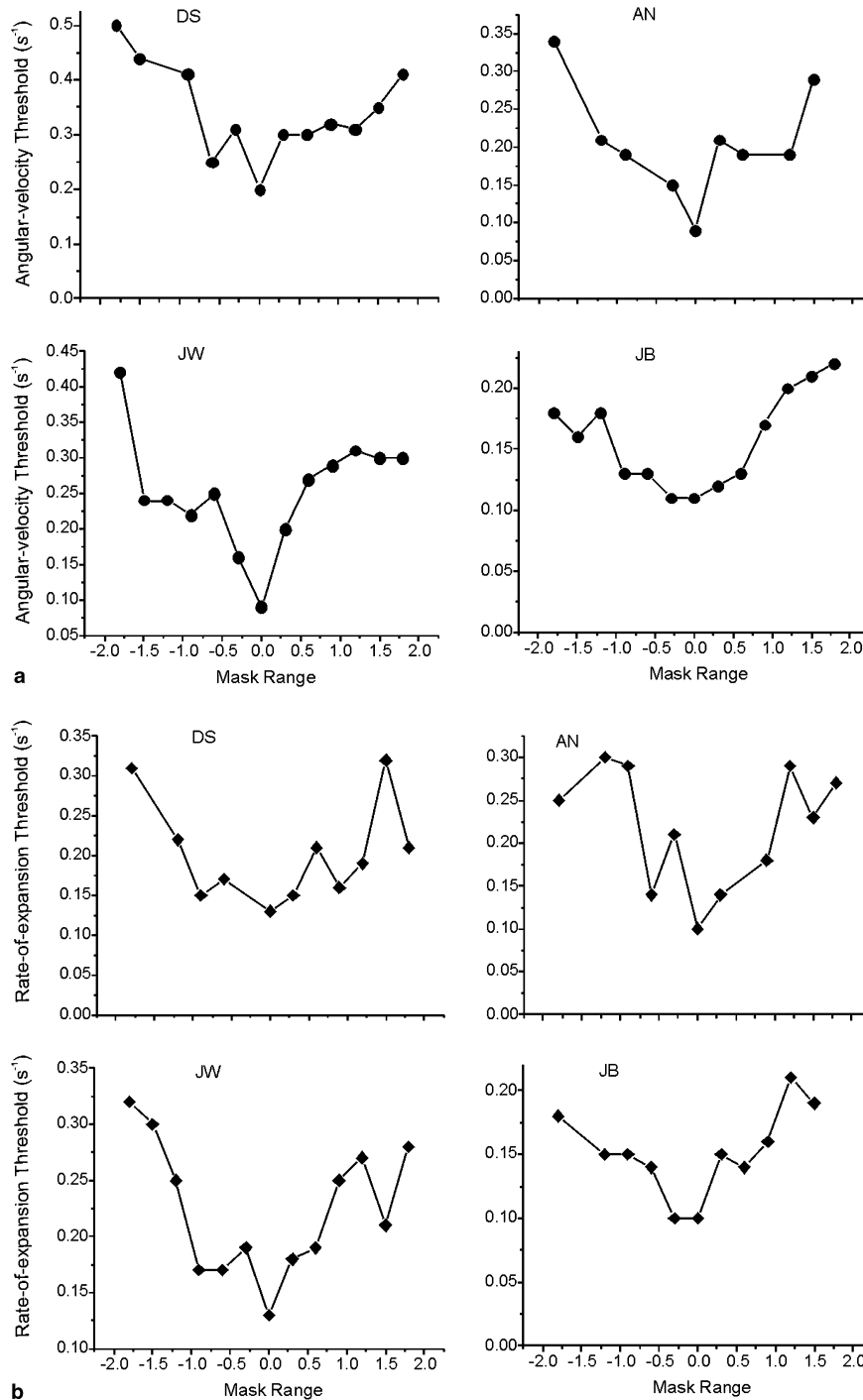


Fig. 4. Motion-rate discrimination threshold as a function of the mask range for four subjects. In (a, b), rotation and radial motion are the components of interest, respectively. The plots show that the discrimination threshold increases with the mask range for both conditions in the same way.

experiment also tested whether averaging hides a small bias as described above. In the experiment, the mask was only applied to the test stimulus and had a fixed value. Fig. 3 shows the bias as a function of the mask value, when the motion of interest is rotation (top) or radial motion (bottom). This figure confirms the results of the first experiment. Furthermore, in the new, control experiment, we tested several values of the mask and found that no bias appears at least up to a mask that is twice the component of interest.

The independence in the estimate of the radial and rotational components of motion showed in Fig. 2 does not appear in the discrimination threshold. Fig. 4(a) and (b) plot this threshold as a function of the mask range, for angular velocity and rate of expansion, respectively. The discrimination threshold increases with the mask range. In other words, the presence of an orthogonal component reduces the sensitivity for the discrimination of angular velocity and rate of expansion.

4. Model

The increase of the threshold for motion-rate discrimination with mask range challenges the strict independence of the mechanisms measuring the different

components of optic flow. How can these results be explained in terms of motion decomposition? Humans make errors in the discrimination of speed of about 5% for a wide range of velocities (McKee, 1981) and in discrimination of direction of motion of less than 1° to several degrees for short translations (Westheimer & Wehrhahn, 1994). We hypothesize that these errors propagate along the visual system, affecting the estimates of angular velocity and rate of expansion. We next show an analysis of this hypothesis for the case in which rotation is the component of interest and expansion is the mask. The same analysis holds for radial motion.

Fig. 5 shows an instant of a hypothetical dot undergoing spiral motion. The thick vector (V) denotes the instantaneous local velocity of the dot. The thin vectors are the rotational (V_Ω) and radial (V_ρ) components of the spiral motion. In dotted and dashed lines are the errors in speed (ΔV) and direction of motion ($\Delta\theta$), respectively, of the estimate of the local velocity. The error in the estimate of the rotational component is a combination of these errors, i.e.,

$$\frac{\Delta V_\Omega}{V_\Omega} = \frac{\Delta V}{V} \cos \Delta\theta - (1 - \cos \Delta\theta) + \frac{V_\rho}{V_\Omega} \sin \Delta\theta \left(1 + \frac{\Delta V}{V}\right). \tag{1}$$

Because $\Delta V/V \approx 0.05$ (i.e., the Weber fraction is about 5%), we can write to a good approximation

$$\frac{\Delta V_\Omega}{V_\Omega} = -(1 - \cos \Delta\theta) + \frac{V_\rho}{V_\Omega} \sin \Delta\theta. \tag{2}$$

Only the third term of the right-hand side of this equation depends on V_ρ . Hence, the dependence of the rotational-component error (ΔV_Ω) on errors of local velocity is mostly due to uncertainty about the direction of motion ($\Delta\theta$). This dependence is essentially not due to uncertainty about local speed (ΔV).

Therefore, we propose that noise in the estimate of local direction of motion causes the dependence of the angular-velocity threshold on the rate of expansion.

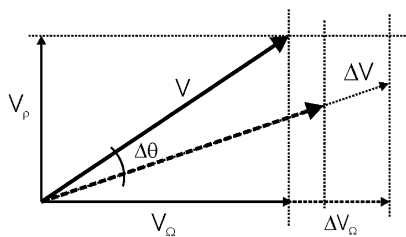


Fig. 5. Schematic of the vector decomposition of the spiral motion (V) into rotation (V_Ω) and radial (V_ρ) motion. The cartoon shows how an error ($\Delta\theta$) in the estimate of direction of the local-velocity vector produces an error in the estimate of the rotational component of the spiral motion. If in addition, one includes the error in local-speed estimation (ΔV), then one obtains the full error of this component (ΔV_Ω).

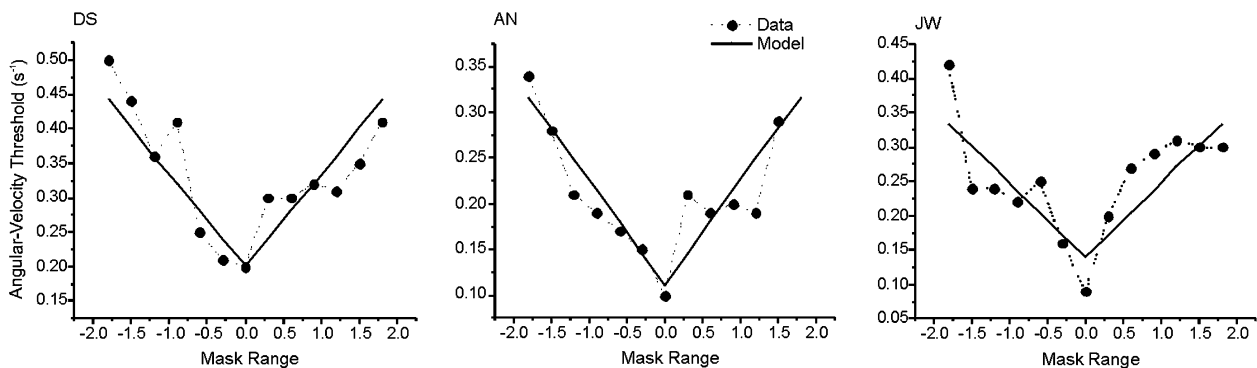


Fig. 6. Model fit of angular-velocity-discrimination threshold as a function of the mask range. The data are for the naïve subjects in Fig. 4 and the plots show how the model fits these data well.

To go from Eq. (2) to errors of angular velocity (Ω), one notes that it is the ratio between the local linear velocity and the distance from the center of rotation. Errors in the estimate of position of dots in our experiments are close to zero. This assumption is valid, since the brain tends to bias the position of the center of rotation towards the fixation point (Barraza & Grzywacz, 2003a, 2003b). And in our experiments, this point coincides with the center of rotation. Consequently, the relative error in the estimate of rotational angular velocity in our experiments is mostly due to the relative error in the estimate of the local velocities (Eq. (2)). To this error, one must add a final error that is due to the computation of angular velocity itself. As with other computations of the visual system, we assume that this latter error is multiplicative (Bowne, McKee, & Glaser, 1989). In other words, this error yields a constant Weber fraction. If one assumes that this fraction and $\Delta V_{\Omega}/V_{\Omega}$ from Eq. (2) are small, then

$$\frac{\Delta\Omega}{\Omega} \cong \frac{\Delta V_{\Omega}}{V_{\Omega}} + \varepsilon, \quad (3)$$

where ε is a constant.

Fig. 6 shows the excellent optimal fits of Eqs. (2) and (3) to the experimental data in Fig. 4 on angular-velocity-discrimination threshold. The optimization was performed over $\Delta\theta$ and ε . The standard deviations of the directional noise ($\Delta\theta$) predicted by the model were 20° for Subject DS, 15° for AN, and 16° for JW. These values were in good agreement with other experiments in the literature (Section 6). In turn, the predicted values of ε were 0.20 for DS, 0.11 for AN, and 0.14 for JW.¹ Again, these estimated values of ε were like those from many other discrimination tasks in vision (Levi & Klein, 1992; Westheimer, 1999).

5. Test

Fig. 6 and the good quality of its fitting parameters suggest that local directional errors may underlie the dependence of angular-velocity-discrimination thresholds on rate of expansion. However, it would be better if our hypothesis on the role of directional errors made a surprising, independent new prediction. And hopefully, it should be testable with available experimental techniques.

We tested the model by measuring discrimination thresholds for pure rotations. These rotations contained

an independent external noise in the direction of motion of each dot. We developed the following two predictions for this external-noise test: First, the external noise should increase the effects of the visual system's internal noise in a predictable, parameter-free manner. If the external and internal noises add independently, then the effective error in local direction of motion is

$$\Delta\theta = (\Delta\theta_E^2 + \Delta\theta_I^2)^{1/2}, \quad (4)$$

where the subscripts E and I refer to external and internal noise, respectively. Because there is no expansion in the stimulus, we can compute the total error due to the effective noise by setting $V_{\rho} = 0$ in Eq. (2). Then, by substituting Eq. (4) for $\Delta\theta$ in Eq. (2), we obtain the predicted error for the new experiment. This prediction is parameter-free, since we set $\Delta\theta_I$ from Fig. 6 and $\Delta\theta_E$ is our independent experimental variable. Second, we predict that external noise in the local direction of motion will produce an underestimation of the angular velocity of the noisy stimulus compared to the non-noisy one. This is because optimal angular velocity is computed from the projection of local velocity onto an axis perpendicular to the line linking the dot to the center of rotation (Barraza & Grzywacz, 2003a, 2003b). Because in a pure rotation, velocities without noise are on this axis, they rotate away from it with noise, yielding smaller projections. Those diminished projections bias the estimated angular velocity towards lower values. We express this bias as the ratio between the estimated angular velocities of the noisy and the non-noisy stimuli:

$$\text{Bias} = \frac{\cos((\Delta\theta_E^2 + \Delta\theta_I^2)^{1/2})}{\cos(\Delta\theta_I)}. \quad (5)$$

As with the first prediction, this second one is parameter-free.

Fig. 7 tests the first prediction by plotting the discrimination threshold for rotational motion as a function of the standard deviation of the external directional noise. The symbols represent the experimental data and the solid lines represent the model predictions. These lines were obtained by plugging into Eqs. (2)–(4) the values of standard deviation of the directional noise $\Delta\theta_I$ and final error (ε) obtained from Fig. 6. Fig. 7 (top panels) shows that the model fits the data well despite being parameter free. To assess the goodness of these fits, we plotted (Fig. 7, bottom panels) the angular-velocity thresholds predicted by the model against those obtained experimentally. A perfect fit of the model would result in a straight line with zero intercept and a slope of one in this plot. To test whether the slope and intercept deviated significantly from the predicted values, we performed a linear regression. From it, we obtained that the probability

¹ These subjects were naïve. In contrast, Subject JB in Fig. 4 was one of the authors of this paper and trained extensively with the displays before the experiments. Therefore, it was not surprising that his thresholds were close to 0.1 and did not vary much over the mask range. Hence, although his data revealed an $\varepsilon \approx 0.1$ like other subjects, the relative constancy of these data suggests that people can learn to reduce the effects of directional errors.

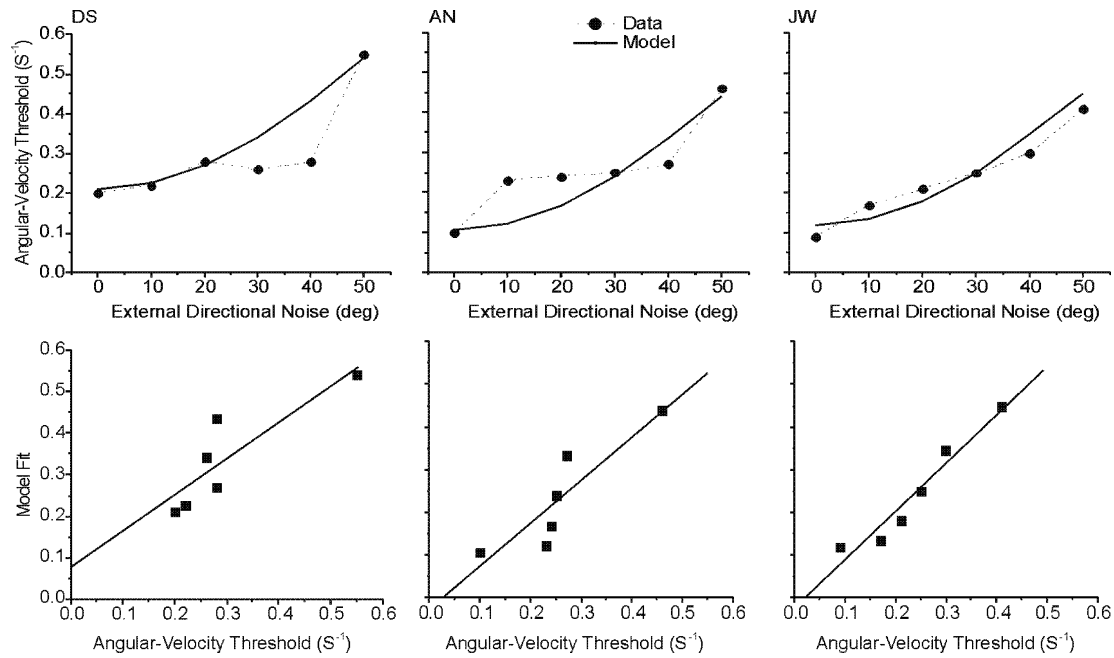


Fig. 7. Test of the model with angular-velocity discrimination-threshold data. *Top panels:* These data as a function of the standard deviation of the external directional noise. The figures plot the discrimination thresholds obtained in a pure rotational-motion display embedded with noise in the direction of the local velocities. Symbols represent the experimental thresholds and solid lines represent the model predictions. The model fits these data well although the simulations were run with values of internal noise obtained from Fig. 6. In other words, these good fits were parameter free. *Bottom panels:* Theoretical versus experimental angular-velocity discrimination threshold. Each square symbol comes from a tested external directional noise in the top panel. Solid lines are regression lines through the square symbols. These lines have intercepts close to the origin and slopes near 1, indicating again that the model is consistent with the data well, fitting them well.

for the line to cross the origin was higher than 40%, 74%, and 55% for Subjects DS, AN, and JW, respectively (two sided *t*-test). Furthermore, the slopes were 0.9 ± 0.2 , 1.0 ± 0.2 , and 1.1 ± 0.1 , and the *R*-squares were 0.75, 0.79, and 0.94, respectively. Therefore, we conclude that the fits in Fig. 7 are not statistically significantly different from the data.

Fig. 8 tests the second prediction by showing the bias as a function of the standard deviation of the external directional noise. Again, the symbols represent experimental data and the solid lines are the model predictions. These predictions were derived from Eq. (5), using $\Delta\theta_1$ estimated from Fig. 6. The plots show that, as predicted, the model underestimates the angular velocity of the noisy stimulus and fits the experimental data well. Hence, the model not only accounts for the original data (Fig. 6) but also for the two new predictions.²

² An alternative to our model may be that the increase of the discrimination threshold is due to interactions between rotational and radial motion components. However, the challenge for such an explanation is to devise interactions that produce such an effect without producing a bias. We propose a simple and biologically plausible explanation that does exactly that.

6. Discussion

We showed that combinations of rotation and radial motion, producing spiral motions, do not induce biases in how humans estimate angular velocity and rate of expansion. This result suggests that the human visual system uses independent mechanisms to measure parameters of these motions accurately. In other words, it seems capable of decomposing complex motion patterns into basic components. Such decomposition is a property of particular theoretical relevance, as raised by the Yuille-and-Grzywacz framework (1998). That the visual system can decompose complex motions supports their theory, which postulates that our brains analyze motion in natural images in large part by means of internal models. These models would include the basic components proposed by Koenderink and van Doorn (1976). However, although motion-parameters estimates appear to be mediated by independent internal models, thresholds for motion-rate discrimination depend on orthogonal components. The sensitivity for motion-rate discrimination decreases with the increase of the mask. Can one interpret this result as evidence that mechanisms measuring the different motion components of optic flow are not independent?

A possible answer begins by considering that angular-velocity and rate-of-expansion mechanisms use common

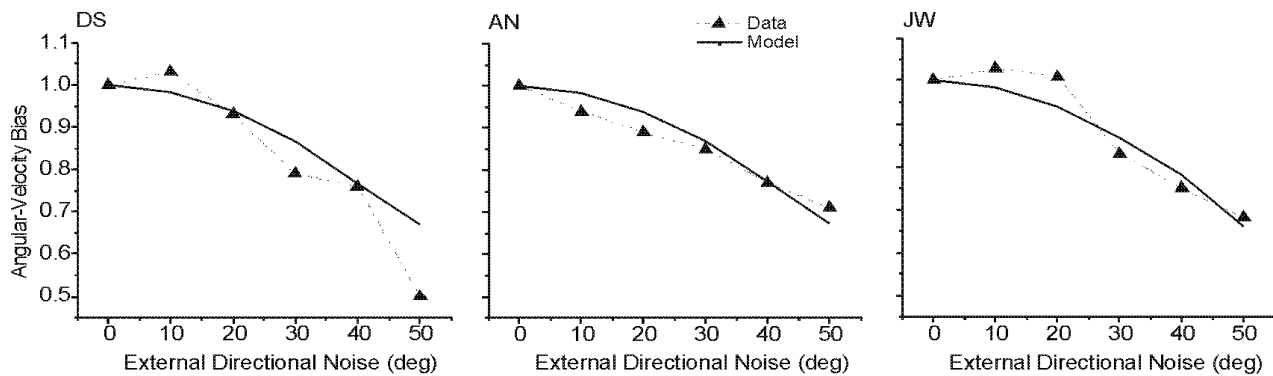


Fig. 8. Angular velocity bias as a function of the standard deviation of the external noise. The bias is the ratio between the perceived angular velocity with and without noise. These results correspond to a pure rotational motion embedded with noise in the direction of the local velocities. As the model predicts (solid lines), subjects underestimate the angular velocity of the noisy versus the noise-free rotation (symbols). Again, this model simulation was parameter free, being performed using the values of internal noise obtained from Fig. 6.

local measurements of linear velocity (Perrone, 1992; Royden, 1997). Therefore, errors in these local measurements can cause statistical correlations in these mechanisms even if they are independent computational processes. We showed how errors in the estimate of local direction of motion can explain errors in the estimate of the basic components of the optic flow. In particular, we could explain errors in optic-flow decompositions (Fig. 6). Moreover, local errors gave rise to surprising results in the estimate of pure-motion components, such as rotation (Figs. 7 and 8). One of the surprises from the fits in Fig. 6 was that, under the present experimental conditions, errors in the estimate of local direction of motion were around 17° (see results after Eq. (3)). This was surprising, since Westheimer and Wehrhahn (1994) showed that humans can discriminate differences in direction of motion as small as 1° . However, these authors also showed that the sensitivity for direction discrimination depended on the spatial excursion of the motion. For example, for an excursion of $40'$, the threshold for discrimination of direction was less than 1° . The threshold then increased rapidly to 3° for excursions of $13'$. In our displays, the mean excursion was $4'$ when considering two frames (one jump) for which the trajectory was rectilinear.³ To evaluate the threshold for this excursion, we inspected Fig. 2 in the Westheimer-and-Wehrhahn article. Extrapolation of their data shows that a 17° threshold may well apply to a $4'$ excursion.

Several previous psychophysical studies addressed the detection of elementary components such as rotation and expansion in complex motion (Freeman & Harris, 1992; Kappers, Te Pas, & Koenderink, 1993). Those studies showed that detection depended more on the direction-of-velocity patterns than on velocity gradients.

Hence, errors in the estimate of local directions may reduce performance for the detection of these components (Kappers et al., 1994). Furthermore, Te Pas et al. (1996) showed that adding a translation to a rotation or an expansion increases the sensitivity to directional noise for direction-discrimination tasks. This effect is stronger when the angular velocity or the rate of expansion decreases. Adding a translation to, for example, a rotation moves its center away from the original position. If only the portion of the image around the former center is displayed, the information of rotation in this area weakens. This is because the deviation from parallel flow decreases (Te Pas et al., 1996). When this deviation decreases so much that it is in the order of the internal directional noise, the performance is strongly affected by an external directional noise. This explains why performance is constant over a range of translational velocities and suddenly falls when this velocity exceeds a given value. This explanation predicts that this range depends on the angular velocity or the rate of expansion as shown in Kappers et al. (1994) and Te Pas et al. (1996). Moreover, the explanation accounts for the effect on detection of rotation or expansion in the presence of the orthogonal component as shown by Te Pas et al. (1996).

What neural mechanisms decompose complex optic flows? Previous studies have shown that the decomposition of spiral motions is probably not performed at the level of a single cell (Orban et al., 1992). The response of a rotation-selective cell decreases substantially when the rotational stimulus is embedded in a radial motion. An alternate strategy would be a population-cell coding. It was found that some cells in area MST of primates are selective to spiral motions (Graziano et al., 1994). We hypothesize that these cells' preferred angular velocity and rate of expansion tile a two-dimensional Cartesian-like space. Each of these variables would define an axis in this space. The angles of its points with respect to one of the axes would indicate the proportion of

³ We considered only two frames, because the total trajectory of a dot, which was three frames long, was not rectilinear and thus, not comparable with Westheimer-and-Wehrhahn data.

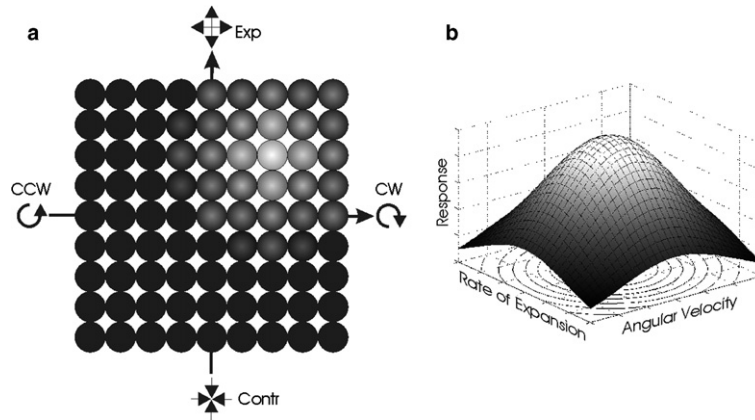


Fig. 9. (a) Schematic of the hypothetical radial-rotational space. While the up and down directions of the schematic correspond to expansions and contractions, respectively, its right and left directions correspond to clockwise and counter-clockwise rotations. Disks represent neurons sensitive to radial, rotational, and spiral motions. The disk centers show preferred angular velocities and rates of expansion. In turn, the gray levels of the disks represent the responses of the cells, with white and black indicating strong and weak responses, respectively. In this example, the stimulus is the spiral motion where parameters are indicated by the coordinates of the white disks. (b) The distribution of responses in (a) as a three-dimensional plot. In this example, the distribution is separable in terms of angular velocity and rate of expansion. Therefore, the estimates of these variables can be given by the distribution of responses along the respective axes.

rotational and radial motion in an optic flow. In turn, the distance from the origin in this space would be proportional to a cell's optimal angular velocity and rate of expansion. In support of this notion, Graziano et al. (1994) found that spiral sensitive cells may constitute a continuum in such a space. We further hypothesize that when a particular combination of rotational and radial motions is presented, a sub-population of the cells would fire. This sub-population would be such that it agglomerates around the coordinate in this space corresponding to the stimulus. The brain may then estimate angular velocity and rate of expansion by projecting the centers of these agglomerations onto the axes of the space. Alternatively, the brain may estimate these parameters by fitting models of rotation and radial motion to the agglomerations (Yuille & Grzywacz, 1998).

Fig. 9 illustrates these ideas by showing a schematic of a hypothetical response distribution of cells in this radial-rotational space and by showing how it may aid in optic-flow decomposition. The gray levels of the disks in Fig. 9(a) represent the amplitudes of the cellular responses. Hence, the cell in white indicates the spiral motion to which the system is responding. Fig. 9(b) shows in a three-dimensional plot a continuum of the distribution of responses to a spiral motion. The plot is truncated to illustrate the response profiles on the axes. If the response distribution were separable in angular velocity and rate of expansion, then these profiles would also present peaks that correspond to the component motion-rates, thus implementing the aforementioned projection to the axes. Therefore, these profiles may encode the angular velocity and rate of expansion of the component motions of the spiral. However, encoding based on axis profiles would not be ideal,

since it would not use much of the neural data in the agglomeration. Moreover, neural responses at the axes would be feeble compared to those near the center of the agglomeration. In contrast, the alternate fitting hypothesis described above would not suffer from these problems, yielding lower estimation errors. This point raises the question of how errors in the estimation of local direction of motion affect a model like that in Fig. 9. The local direction of motion encodes the proportion of the components of a specific spiral motion (Fig. 4). Therefore, spiral-cell responses depend on the noise and directional tuning of the input directionally selective cells. A directional error would broaden the response distribution in the radial-rotational space, making the estimates of the components less precise.

Acknowledgments

We thank Vincent Chen, Fan Liu, David Merwine, Joaquín Rapela, and Jeff Wurfel for discussions during the performance of this work and Lia Diepstraten for administrative support. The work was supported by a CONICET re-entry fellowship, by an ANPCyT Grant PICT03-11687, by a Fundación Antorchas Grant 14306/2 to JB, and by National Eye Institute Grants EY08921 and EY11170 to JB and NMG.

References

- Barraza, J. F., & Grzywacz, N. M. (2002). Measurement of angular velocity in the perception of rotation. *Vision Research*, 42, 2457–2462.

- Barraza, J. F., & Grzywacz, N. M. (2003a). Local computation of angular velocity in rotational visual motion. *Journal of the Optical Society of America A—Optics Image Science and Vision*, *20*, 1382–1390.
- Barraza, J. F., & Grzywacz, N. M. (2003b). Parametric decomposition of complex motion by humans. *Journal of Vision*, *3*(Suppl.), 279a (Abstract).
- Barraza, J. F., & Grzywacz, N. M. (2004). Parametric measurements of optic flow by humans. In L. M. Vaina, S. A. Beardsley, & S. K. Rushton (Eds.), *Optic flow and beyond* (pp. 221–243). Dordrecht, Netherlands: Kluwer Academic Publishers.
- Bowne, S. F., McKee, S. P., & Glaser, D. A. (1989). Motion interference in speed discrimination. *Journal of the Optical Society of America A*, *6*, 1112–1121.
- De Bruyn, B., & Orban, G. A. (1988). Human velocity and direction discrimination measured with random dot patterns. *Vision Research*, *28*, 1323–1335.
- Duffy, C. J., & Wurtz, R. H. (1991a). Sensitivity of MST neurons to optic flow stimuli. I. A continuum of response selectivity to large-field stimuli. *Journal of Neurophysiology*, *65*, 1346–1359.
- Duffy, C. J., & Wurtz, R. H. (1991b). Sensitivity of MST neurons to optic flow stimuli. II. Mechanisms of response selectivity revealed by small-field stimuli. *Journal of Neurophysiology*, *65*, 1346–1359.
- Freeman, T. A. C., & Harris, M. G. (1992). Human sensitivity to expanding and rotating motion: effects of complementary masking and directional structure. *Vision Research*, *32*, 81–87.
- Gibson, J. J. (1950). *The perception of the visual world*. Boston, Massachusetts: Houghton Mifflin.
- Graziano, M. S. A., Andersen, R. A., & Snowden, R. J. (1994). Tuning of MST neurons to spiral motions. *Journal of Neuroscience*, *14*, 54–67.
- Johnston, A., Benton, C. P., & Morgan, N. J. (1999). Concurrent measurement of perceived speed and speed discrimination using the method of single stimuli. *Vision Research*, *39*, 3849–3854.
- Kappers, A. M. L., Te Pas, S. F., & Koenderink, J. J. (1993). Detection of divergence in optic flow fields. *Perception*, *22*(Suppl.), 83a.
- Kappers, A. M. L., van Doorn, A. J., & Koenderink, J. J. (1994). Detection of vorticity in optical flow fields. *Journal of the Optical Society of America A*, *11*, 48–54.
- Koenderink, J. J., & van Doorn, A. J. (1976). Local structure of movement parallax of the plane. *Journal of the Optical Society of America*, *66*, 717–723.
- Lagae, L., Maes, H., Raiguel, S., Xiao, D., & Orban, G. A. (1994). Response of macaque STS neurons to optic flow components: a comparison of areas MT and MST. *Journal of Neurophysiology*, *71*, 1597–1626.
- Levi, D. M., & Klein, S. A. (1992). Weber's law for position: the role of spatial frequency and contrast. *Vision Research*, *32*, 2235–2250.
- Maunsell, J. H. R., & Van Essen, D. C. (1983). Functional properties of neurons in middle temporal visual area of the macaque monkey. I: selectivity for stimulus direction, speed, and orientation. *Journal of Neurophysiology*, *49*, 1127–1147.
- McKee, S. P. (1981). A local mechanism for differential velocity detection. *Vision Research*, *21*, 491–500.
- Meese, T. S., & Harris, M. G. (2001). Independent detectors for expansion and rotation, and for orthogonal components of deformation. *Perception*, *30*, 1189–1202.
- Morrone, M. C., Burr, D. C., & Vaina, L. M. (1995). Two stages of visual processing for radial and circular motion. *Nature*, *376*, 507–509.
- Orban, G. A., Lagae, L., Verri, A., Raiguel, S., Xiao, D., Maes, H., et al. (1992). First-order analysis of optical flow in monkey brain. *Proceedings of the National Academy of Sciences*, *89*, 2595–2599.
- Perrone, J. A. (1992). Model for the computation of self-motion in biological systems. *Journal of the Optical Society of America A*, *9*, 177–194.
- Regan, D., & Beberley, K. J. (1978). Looming detectors in the human visual pathway. *Vision Research*, *18*, 415–421.
- Regan, D., & Beberley, K. J. (1985). Visual responses to vorticity and the neural analysis of optic flow. *Journal of the Optical Society of America A*, *2*, 280–283.
- Royden, C. S. (1997). Mathematical analysis of motion-opponent mechanisms used in the determination of heading and depth. *Journal of the Optical Society of America A*, *14*, 2128–2143.
- Snowden, R. J., & Milne, A. B. (1995). The effects of adapting to complex motions: position invariance and tuning to spiral motions. *Journal of Cognitive Neuroscience*, *8*, 435–452.
- Tanaka, A., Fukuda, Y., & Saito, H. (1989). Underlying mechanisms of the response specificity of expansion/contraction, and rotation cells, in the dorsal part of the medial superior temporal area of the macaque monkey. *Journal of Neurophysiology*, *62*, 642–656.
- Tanaka, A., & Saito, H. (1989). Analysis of motion of the visual field by direction, expansion/contraction, and rotation cells clustered in the dorsal part of the medial superior temporal area of the macaque monkey. *Journal of Neurophysiology*, *62*, 626–641.
- Te Pas, S. F., Kappers, A. M. L., & Koenderink, J. J. (1996). Detection of first-order structure in optic flow fields. *Vision Research*, *36*, 259–270.
- Westheimer, G. (1999). Discrimination of short time intervals by the human observer. *Experimental Brain Research*, *129*, 121–126.
- Westheimer, G., & Wehrhahn, C. (1994). Discrimination of direction of motion in human vision. *Journal of Neurophysiology*, *71*, 33–37.
- Wurfel, J. D., Barraza, J. F., & Grzywacz, N. M. (2003). Measurement of rate of expansion in the perception of radial motion. *Journal of Vision*, *3*(Suppl.), 399a (abstract).
- Yuille, A. L., & Grzywacz, N. M. (1998). A theoretical framework for visual motion. In T. Watanabe (Ed.), *High-level motion processing—Computational, neurobiological, and psychophysical perspectives* (pp. 187–211). Cambridge, Massachusetts: MIT Press.